Loss of histone H4K20 trimethylation occurs in preneoplasia and influences prognosis of non-small cell lung cancer

Arnaud van den Broeck, Elisabeth Brambilla, Denis Moro-Sibilot, Sylvie Lantuejoul, Christian Brambilla, Béatrice Eymin, Saadi Khochbin, Sylvie Gazzeri

Loss of histone H4K20 trimethylation occurs in preneoplasia and influences prognosis of non-small cell lung cancer

Arnaud Van Den Broeck[1,2], Elisabeth Brambilla[1,2,4], Denis Moro-Sibilot[1,2,3], Sylvie Lantuejoul[1,2,4], Christian Brambilla[1,2,3], Beatrice Eymin[1,2], Saadi Khochbin[2,5] and Sylvie Gazzeri[1,2]

[1] Equipe Bases Moléculaires de la Progression des Cancers du Poumon, Centre de Recherche INSERM U823, Institut Albert Bonniot, 38042 Grenoble Cedex 09, France, [2] Université Joseph Fourier, 38041 Grenoble Cedex 09, France, [3] Pole de Médecine Aigue Communautaire. Pneumologie, Hôpital Albert Michalon, BP217, 38043 Grenoble Cedex 09, France, [4] Departement d'Anatomie et Cytologie Pathologique, Hôpital Albert Michalon, BP217, 38043 Grenoble Cedex 09, France, [5] Equipe Epigénétique et signalisation cellulaire, Centre de Recherche INSERM U823, Institut Albert Bonniot, 38042 Grenoble Cedex 09, France,

Grant support: Institut National de la Sante et de la Recherche Medicale U823, La Ligue Nationale Contre le Cancer (Equipe Labellisée), INCa (Programme National d'Excellence Spécialisé, 2005-2007), PHRC 2004-2007 Micromethods in Pathology. This work was also supported by EpiPro network (SG and SK) supported by INCa and by EpiMed program (Grenoble plateforme) supported by Rhône-Alpes cancéropôle (CLARA).

Request for reprints:

Sylvie Gazzeri

Equipe Bases Moléculaires de la Progression des Cancers du Poumon, Centre de Recherche

INSERM U823, Institut Albert Bonniot BP170, 38042 Grenoble Cedex 09 France

Phone: 33 4 76 54 94 76, Fax: 33 4 76 54 94 13, Sylvie.Gazzeri@ujf-grenoble.fr

Running Title: Loss of histone H4K20 trimethylation in lung cancer

Key words: epigenetic, acetylation, methylation, histone H4, lung cancer

Statement of clinical relevance:

In spite of diagnosis and treatment improvements, lung cancer is the leading cause of death from cancer with a 10 years overall survival less than 10%. Although surgical resection of lung tumors restricted to the chest is in many cases the most effective method to control the disease, it might not be sufficient or curative for a proportion of patients with stage I NSCLC as inferred from 30% death within 5 years after surgery. The use of adjuvant chemotherapy is still a matter of debate for these patients. Several highthrouput analyses have suggested that stage I NSCLC might represent heterogeneous prognostic subgroups. In this study, by using a simple immunohistochemical approach with a specific antibody, we demonstrate that the status of histone H4K20 trimethylation stratifies patients with stage I adenocarcinoma tumors for risk of cancer death. Therefore, studying H4K20me3 status might represent a useful genomic tool to identify prognostic subgroups of stage I patients that could justify the use of adjuvant chemotherapy.

Abstract

Purpose: Epigenetic modifications of Histones have crucial roles in the control of gene activity, nuclear architecture and genomic stability. In this respect they may contribute to the development and progression of cancer. We investigated whether epigenetic changes of histone H4 are involved in lung carcinogenesis.

Experimental design: Epigenetic modifications of histone H4 were studied by immunohistochemistry (IHC) in normal lung and 157 lung carcinoma using antibodies specifically recognizing the acetylated (Ac) lysines 5 (K5), K8, K12, K16 and trimethylated (me3) K20 residues of histone H4. Western blotting was used to validate the IHC results. H4K20me3 was also studied in 17 preneoplastic lesions. Expression of the Suv4-20h1/2 trimethyltransferases was analyzed by quantitative RT/PCR in a subset of tumor samples.

Results: As compared to normal lung, cancer cells displayed an aberrant pattern of histone H4 modifications with hyperacetylation of H4K5/K8, hypoacetylation of H4K12/K16 and loss of H4K20 trimethylation. Alteration of H4K20 trimethylation was frequent in squamous cell carcinoma (67%) and was observed in early precursors lesions in which the level of H4K20me3 staining strongly decreased with disease progression. In adenocarcinoma, the downregulation of H4K20me3 was less frequent (28%) but allowed the identification of a subgroup of stage I adenocarcinoma patients with reduced survival (p=0.007). Loss of H4K20 trimethylation was associated with decreased expression of Suv4-20h2, a specific H4K20 trimethyltransferase involved in telomere length maintenance.

Conclusions: Our findings indicate an important role of histone H4 modifications in bronchial carcinogenesis and highlight H4K20me3 as a candidate biomarker for early detection and therapeutic approaches of lung cancer.

Introduction

Lung cancer is the leading cause of death from cancer among males in Europe and both men and women in the USA. Non-small-cell lung cancer (NSCLC) accounts for almost 80 percent of such deaths (1-3). In spite of diagnosis and treatment improvements, 10 years overall lung cancer survival is less than 10%, claiming more deaths than breast, colon and prostate cancers all together. Early diagnosis allowing surgical resection with a 60 to 80% 5 years survival is performed in only less than 25% of the patients. Therefore, the identification of the molecular biomarkers of clonal selection in lung cancer as well as the comprehension of the mechanisms of their participation to the lung carcinogenesis process are required to establish the prognostic factors of progression of preneoplastic and invasive tumors towards earlier diagnosis, and to define more efficient therapies with lower side effects.

Lung cancer is the end result of a process that associates multifocal morphological transformation and multistep accumulation of molecular abnormalities (4). The clonal selection leading to proliferation and invasion is achieved by disruption of the cell growth controls, with a tumor progression kinetic depending on the number and accumulation rate of these molecular alterations. Common genetic abnormalities in lung carcinogenesis include invalidation of tumor suppressor genes, activation of oncogenes and chromosomal abnormalities (5). Furthermore, it is now apparent that epigenetic modifications that do not affect the primary sequence of the DNA also contribute to lung tumor formation. These involve both global genomic hypomethylation leading to chromosomal instability, and regional hypermethylation at certain promoters (6-8). By this mechanism of silencing, the expression of tumor suppressor genes in the cancer cell can be reduced or eliminated as an alternative mechanism to genetic mutation. Chromatin modifications represent another mechanism of epigenetic regulation. They occur at the level of histones that are the targets for several post-translational covalent modifications which allow regulable contacts with the

underlying DNA and thus affect higher-order chromatin structures (9). In this regard, histone covalent modifications influence a multitude of cellular processes (10-12) and aberrant histone acetylation and methylation patterns were recently reported in human tumors (13, 14). Histone H4 is one of the nucleosomal core histones. Acetylation and methylation of lysine residues in its N-terminal tail have been reported to affect higher-order chromatin structure, transcriptional regulation and DNA repair, suggesting that alteration of these histone marks might play a role in tumorigenesis (12). Accordingly, loss of lysine 16 acetylation and lysine 20 trimethylation has been recently shown in cancer cells from liver, breast and colon as well as in lymphoma (1, 14, 15). The aim of this study was to analyze the role of histone H4 modifications in lung cancer. We examined the acetylation and methylation pattern of histone H4 in human normal lung and non small cell lung cancer by using immunohistochemistry and specific antibodies, and analyzed the relationships with clinico-parameters and clinical outcome. Our results demonstrate a global distorted pattern of histone H4 modifications in lung tumors and provide evidence that loss of H4K20 trimethylation plays a crucial role in lung tumorigenesis.

Materials and methods

Patients and tissue samples

Patient selection was based on consecutive collection of cases in the tumor bank balanced between histo-pathological subtypes, and completeness of clinical data (date and cause of death, at least 5 years of follow up, absence of chemotherapy given before or after surgical resection). One hundred and fifty seven human lung tumors were included in this study. Tissue samples were taken at surgical resection of lung tumors in all cases. Tumor tissue and normal lung parenchyma taken at distance from the bulk of the tumor were immediately frozen and stored at -80°C until use. For histological classification, tumor

samples were fixed in formalin and diagnosis was made on paraffin-embedded material using the current World Health Organization International Classification of lung criteria (16). They consisted of 50 squamous cell carcinoma (13 stage I, 11 stage II, 25 stage III and 1 stage IV) and 107 adenocarcinoma (80 stage I, 7 stage II, 17 stage III and 3 stage IV). Tumors were used according to the ethical laws of our country. The median time of follow up calculated by the Schemper and Smith method (17) was 67 months. Bronchial intraepithelial preinvasive lesions were obtained from lung resection performed for lung cancer in 7 patients. Preinvasive lesions were classified according to the WHO classification criteria (16). Squamous metaplasia and mild dysplasia were considered as low-grade dysplasia, whereas moderate dysplasia, severe dysplasia and CIS were considered as high-grade dysplasia.

Immunohistochemistry

Seven-micrometer-thick serial frozen sections were incubated at 42°C with primary antibodies anti-acetylated H4K5 (Abcam ab1758, 1/100), anti-acetylated H4K8 (Abcam ab1760, 1/2000, anti-acetylated H4K12 (Upstate 06-761, 1/750), anti-acetylated H4K16 (Abcam ab1762, 1/400) and anti-trimethylated H4K20 (Upstate 07-463, 1/800). Fixation was with 3.7% paraformaldehyde for 10 minutes. A three-stage indirect immunoperoxidase technique was performed using the Ventana Discovery Autostainer (Ventana Medical International Inc.Tuscon, AZ, USA) which garanties full reproducibility of immunostaining. Negative control consisted in omission of the primary antibody and incubation with immunoglobulins of the same species and isotype. Immunostaining was performed on whole sections and evaluated independently by two pathologists (EB, SL) who were blinded to all clinico-pathological variables (E.B, S.L). Selectivity and validation of the antibodies was ensured by recognition of different pattern of stained cells for H4K5Ac/K8Ac/K12Ac/K16Ac/K20me3 on serial sections of 3 microns intervals, as well as

on tumor blots. Reproducibility of staining was validated in 10 cases stained at several days interval times : the variability between the two score assessments by pathologists was less than 10% of global score. Scores of staining were ascribed to each case and antibody by multiplying the percentage of positive cells (0 to 100%) by the staining intensity (0, null; 1, faint; 2, moderate; 3, strong). They ranged from 0 to 300. Normal bronchi and alveolar epithelial cells were used as positive internal controls. These normal structures exhibited low staining scores for acetylated H4K5/K8 (20 and 40 respectively) and high staining scores for acetylated H4K12/16 and trimethylated H4K20 (300, 240 and 250 respectively).

Immunoblotting

Immunoblotting was performed on 15 representative tumor samples and their matched normal lung tissues. Proteins were extracted from sections taken at the immediate vicinity of those studied by immunohistochemistry. Immunoblotting experiments were performed as previously described (18) with the same antibodies used for immunohistochemistry. Dilutions of the primary antibodies were 1:500 for acetylated H4K5 and 1/1000 for acetylated H4K8/K12/K16 and trimethylated H4K20 antibodies. To ensure equal loading and transfer of proteins, the membranes were subsequently probed with a polyclonal actin antibody (1:500; Sigma-Aldrich; L'Isle d'Abeau).

RT-QPCR

Total RNA was extracted from normal and human lung tumors samples using RNeasy Mini Kit (Qiagen), according to the manufacturer's instructions. RNA concentration was determined using Eppendorf Biophotometer AG22331 (Hamburg, Germany) and RNA integrity was assessed using the Agilent Bioanalyzer 2100 (Agilent Technologies, Waldbronn, Germany). Quantitative real-time RT-PCR for Suv4-20H1 and Suv4-20H2

mRNA (genbank acc. no. NM_017635 and NM_032701) was performed on Stratagene MX3005P apparatus. 1µg of total RNA were subjected to cDNA synthesis with Superscript III First-Strand Synthesis SuperMix for qPCR (Invitrogen) and subsequently amplified during 40 PCR cycles (10 min at 95°C, cycles: 15 s at 95°C, 1 min at 60°C) using Power SYBR Green PCR Master Mix (Applied Biosystems) The specific primers used for mRNA amplification were as follows: Suv4-20H1 forward: 5'- CGC CCT GCA CCT ACA TAA CT-3'; reverse: 5'-ACA CTT TGC CTC CCC TTT TT-3'; Suv4-20H2 forward: 5'-CGG TGA GAA TGA CTT CAG CA-3'; reverse: 5'-CTC ACA GGT GTG GCA TTC AC. In parallel, RT-PCR detecting the reference gene Glyceraldehyde-3-Phosphate Deshydrogenase (GAPDH) was performed for each sample. Relative gene expression was calculated for each sample, as the ratio of Suv4-20H1 or Suv4-20H2 copy number (target gene) to GAPDH mRNA copy number multiplied by 100, thus normalizing Suv4-20H1 or Suv4-20H2 mRNA expression for sample to sample differences in RNA input.

Statistical analyses

To test whether variables were correlated within patients, we used the Spearman test. Descriptive analyses comparing continuous and two-level categorical variables were carried out using Mann Whitney test. The chi-2 test was used to test the association between two categorical variables. Overall survival was calculated from the date of surgery to the last day of follow-up or cancer death. Univariate survival analyses were performed using the Kaplan-Meier method and the log-rank test. Statistics were performed using Statview 4.1 software (Abacus Concept Inc, Ca). A p-value of less than 0.05 was considered statistically significant.

Results

Global modification of histone H4 acetylation in lung cancer

One hundred non small cell lung cancers comprising 50 squamous carcinoma and 50 adenocarcinoma were analyzed by immunohistochemistry (IHC) using antibodies specifically recognizing the acetylated (Ac) lysines 5 (K5), K8, K12 or K16 residues of histone H4. Low levels of nuclear H4K5Ac and H4K8Ac staining were found in normal lung parenchyma adjacent to or distant from tumor bulk, whereas high levels of immunostaining were observed for H4K12Ac and H4K16Ac (Figure 1 and supplementary Figure 1). Therefore, these data show that the lysine residues of the H4 tail exhibit a differential pattern of acetylation in the normal lung.

As compared to normal lung parenchyma, the study of lung tumors revealed a general increase of H4K5Ac/K8Ac expression (Figure 1, panels a and b) and decrease of H4K12Ac/16Ac expression (Figure 1, panels c and d). The IHC data were validated for each antibody by immunoblotting in 15 representative tumor samples and their matched normal lung tissues. Figure 1 (middle) illustrates an example of the results. As compared to normal lung, acetylation of H4K16 was clearly downregulated in lung tumors with more than 70% of samples displaying a score between 0 and 100 (Figure 1, right panel). Distribution of H4K16Ac staining was very similar between both histological types (Figure 2). By contrast, a broader distribution of H4K5Ac, H4K8Ac and H4K12Ac stainings was observed. Furthermore, high levels of H4K5Ac and H4K8Ac were more frequent in squamous cell carcinoma whereas low levels of H4K12Ac were predominantly observed in adenocarcinoma (Figure 2, Mann Whitney, $p=0.016$, $p<0.0001$ and $p=0.0007$ respectively). A strong association between H4K8Ac and H4K12Ac was observed in squamous cell carcinoma (Spearmann's correlation coefficient, $r=0,6038$; $p<0.0001$) whereas H4K12Ac and H4K16Ac

were correlated in adenocarcinoma (Spearmann's correlation coefficient, r=0,49; p=0.0009). A strong association between H4K5Ac and H4K8Ac (Spearmann's correlation coefficient, r=0,409; p<0.0001) or H4K5Ac and H4K12AC (Spearmann's correlation coefficient, r=0,347; p=0.0007) was also found independently of the histological type. The significance of these correlations is still unclear but could reflect a thorough crosstalk between histone H4 modifications as recently described for histone H3 (19, 20). No additional significant relationships were observed between H4K5/K8/K12/K16Ac stainings and clinico-parameters (stage, clinical outcome).

Loss of trimethylation at H4K20 in lung tumors.

The same series of lung carcinoma was studied for histone H4 lysine 20 trimethylation (H4K20me3) by immunohistochemistry using a specific anti- trimethylated K20 antibody. As shown in Figure 3A, a global loss of H4K20me3 was observed in lung tumors (panel b) as compared to normal lung that expressed strong H4K20me3 staining (panel a). These results were confirmed by western blotting in representative cases (Figure 3B). The distribution of H4K20me3 staining scores showed that 70% of the tumor samples had a H4K20me3 score between 0 and 100 (Figure 3C). As the mean score of the normal lung was 250, it can be stated that trimethylation of H4K20 is frequently and strongly decreased in lung tumors. Strikingly, loss of H4K20me3 was more frequent in squamous carcinoma than in adenocarcinoma (Figure 3D, Mann Whitney, p<0.0001). Moreover, a strong inverse association between H4K8Ac and H4K20me3 modifications was detected in adenocarcinoma (Spearmann's correlation coefficient, r=-0.487; p=0.0008).

Trimethylation at H4K20 is lost in squamous preneoplasia.

Trimethylation of H4K20 was strongly downregulated in squamous carcinoma as revealed by the distribution of H4K20me3 scores (67% of cases with a score <60, Figure 3D and 4A). In these tumors, no relationship was observed between H4K20me3 IHC status and stage or clinical outcome but we noticed that a large proportion (69%) of stage I tumor samples exhibited very low levels of H4K20me3 (score<60). This led us to investigate the possibility that this histone modification could take place early during squamous carcinogenesis. Stepwise morphological changes accompanying this transformation process have been described in smokers and include squamous hyperplasia (H), metaplasia (M), dysplasia (D) of progressive severity (mild, moderate and severe) and carcinoma in situ (CIS) (21). According to the criteria provided by the WHO classification of lung cancers and precursors, metaplasia, dysplasia and CIS represent preinvasive lesions of the bronchial epithelium (16) whereas basal hyperplasia are very common reactive lesions in adults. To assess whether loss of trimethylation at H4K20 might be involved in the development of squamous cell carcinoma, we analyzed its IHC status in a series of 18 preinvasive lesions observed in 7 surgical resection frozen specimens for cancer. They consisted of 4 basal hyperplasia, 4 metaplasia, 2 mild dysplasia, 2 moderate dysplasia, 2 severe dysplasia and 4 CIS. As compared to normal bronchial epithelium in which basal cells exhibited a strong nuclear staining, we noticed that hyperplasia displayed a less intense H4K20me3 immunostaining with the appearance of some negative nuclei. Strikingly, the level of H4K20me3 strongly decreased with disease progression from cell hyperplasia to metaplasia, dysplasia (mild, moderate, severe) and then to CIS (Figure 4, B and C). Therefore, these results demonstrate that trimethylation of H4K20 is lost in early precursors lesions of squamous cell carcinoma.

Loss of H4K20me3 correlates with a poor survival in stage I adenocarcinoma patients

In contrast with squamous cell carcinoma, the downregulation of H4K20me3 was less frequent in adenocarcinoma (28% of cases with a score <60, Figure 3D). Interestingly, the distribution of H4K20me3 scores clearly identified two populations of stage I adenocarcinoma tumor samples with distinct clinical outcome, a longer cancer related survival being observed for patients whose tumors expressed higher levels (score > 100) (Figure 5A, p=0.0125). To validate the prognostic power of H4K20me3 in early stage adenocarcinoma, we studied H4K20me3 immunostaining in another set of stage I adenocarcinoma. Analysis of these new series of 57 stage I adenocarcinoma samples confirmed the existence of two distinct H4K20me3 staining groups (Figure 5B). According to Kaplan-Meier analysis recording cancer related death, 30% of low H4K20me3 staining carriers (score ≤ 100) had died from lung cancer at 5 years after diagnosis compared with 5% of noncarriers. The median survival time for low H4K20me3 carriers was 114 ± 2.8 months, whereas it was not reached for patients who had high H4K20me3. Therefore, carrying low levels of H4K20me3 was associated with reduced survival for patients with stage I adenocarcinoma as compared to cases with high levels of H4K20me3 (p = 0.024). Finally, the influence of loss of H4K20 trimethylation was evaluated on the all stage I population combining test series and validation cases. In this population of 80 stage I adenocarcinoma, the median survival time was 140 ± 4 months. The results showed that low H4K20me3 staining correlated with shorter cancer related survival (median 114 ± 2.8) as compared to cases with high H4K20me3 staining (median non reached, p=0.007). Age (<60 years versus >60 years), sex (male versus female) and T stage (IA versus IB) were not associated with survival in univariate analyses. Thus, we did not associate these variables to H4K20me3 in a multivariate Cox proportional hazard model.

Loss of Suvar4-20h2 expression correlates with reduced H4K20me3

Mechanistic basis of H4K20me3 modification may be related to altered expression of various histone-modifying enzymes. Enzymes that demethylate H4K20 have not yet been identified. By contrast, it is well-known that trimethylation of histone H4 lysine 20 is catalysed by the histone methyltransferases (HMTases) Suv4-20h1/2 (also called KMT5B/C) (22). To uncover the mechanisms involved in H4K20me3 deregulation in lung tumors, we analyzed the expression of suvar4-20h1/2 HMTases. Because available Suv4-20h1/2 antibodies did not work for immunohistochemical application in our hands, we performed quantitative RT/PCR analysis. Total RNA was extracted from 31 representative tumor samples exhibiting either very low ($\leq$ 60) or very high ($\geq$210) scores of H4K20me3 according to IHC, as well as from their matched normal lung. Tumors were considered having an altered expression of Suv4-20h1 or Suv4-20h2 when a modification of at least 50% of the transcript level was observed as compared to matched normal lung. The data showed that 68% (21/31) and 55% (17/31) of tumor samples had a decreased level of Suv4-20h1 and Suv4-20h2 transcripts respectively as compared to normal lung (Table 1), thereby indicating that expression of Suv4-20h transcripts is globally downregulated in lung tumors. Importantly, we observed that low levels of H4K20me3 were associated with a decrease of Suv4-20h2 transcripts ($p=0.019$). By contrast, no significant association was found between H4K20me3 staining and Suv4-20h1 mRNA level ($p=0.37$). Altogether these results suggest that alteration of Suv4-20h2 expression might play a role in the deregulation of H4K20 trimethylation in lung tumors.

Discussion

The prognosis of lung cancer is affected by the difficulties of diagnosing early stage disease amenable to surgery. Thus, novel diagnostic, risk assessment and therapeutic

approaches are urgently needed for this common and devastating cancer. Epigenetic has become an increasingly important aspect of cancer biology. Epigenetic changes encompasse an array of molecular modifications to both DNA and chromatin, the most extensively investigated of which is DNA methylation. Recently, aberrant histone acetylation and methylation patterns have been reported in tumors (13, 14), suggesting that perturbation in chromatin structure may also contribute to tumorigenesis. In this study, we show that lung tumors exhibit an altered pattern of histone H4 modifications as compared to normal lung. Furthermore, we demonstrate that trimethylation at lysine 20 of histone H4 is dramatically reduced in squamous preneoplastic lesions and provide evidence that loss of H4K20me3 predicts a bad prognosis for patients with early stage adenocarcinoma. Altogether, our results highlight the role of chromatin disorders in lung carcinogenesis and support the idea that post-translational modifications of histone H4 are relevant steps in the lung transformation process.

It is becoming clear that aberrant modification of histones can play a major role during the multistep process of cancer development. In this study we show that human lung tumors display a clear downregulation of H4K20 trimethylation. As loss of H4K20 trimethylation has been reported in lymphoma, colon and breast cancer as well as in various cancer cell lines (14, 15), our results are consistent with the notion that aberrant H4K20me3 is a common hallmark of human cancer. Adenocarcinoma and squamous carcinoma are the main histological subtypes of non-small-cell lung cancer. They can be distinguished not only on the basis of pathological features but also by distinct molecular alterations that contribute to their development. This is best illustrated by the quite selective occurrence of Ras and EGFR mutations in adenocarcinoma (5). In this study, we demonstrate that aberrant H4K20 trimethylation is frequent in squamous carcinoma and occurs early in preneoplastic precursors lesions in which the level of H4K20me3 strongly decreases along the sequential progression from cell hyperplasia to metaplasia, dysplasia and then to carcinome in situ. In contrast,

whereas altered trimethylation of H4K20 is less frequent in adenocarcinoma, it was found to influence the disease outcome. Altogether, these data support the idea that aberrant trimethylation of H4K20 might play a role in the early steps of squamous carcinoma development, whereas it could contribute to the progression and aggressivity of adenocarcinoma. However, we have not excluded the possibility that atypical adenomatous hyperplasia, the precursors lesions of adenocarcinoma with bronchioloalveolar features, display loss of H4K20 trimethylation. These lesions are not available in frozen lung tissue, a requirement for our antibody performance.

The mechanism involved in the loss of H4K20me3 is not yet elucidated. Two histone methyltransferases (HMTases), namely Suv4-20h1/2, are responsible for H4K20 trimethylation (22). Importantly, we demonstrate that loss of H4K20me3 is associated with a decrease of Suv4-20h2 transcripts. These data suggest that disruption of Suv4-20h2 expression might contribute to altered H4K20me3 pattern at least in lung tumors. Although we cannot exclude the possibility that yet unidentified demethylase(s) specific for H4K20me3 might be abnormally expressed in cancer cells, it is important to notice that similar correlation between H4K20me3 and Suv4-20h2 expression has been previously reported in human breast cancer cell lines as well as in a model of hepatocarcinogenesis induced by methyl deficiency in rats (1, 15).

Approximately 45% of all lung carcinoma are limited to the chest, where surgical resection is not only an important therapeutic modality, but in many cases, the most effective method to control the disease. However, surgical treatment might not be sufficient or curative for a proportion of patients with NSCLC and especially adenocarcinoma, as inferred from 30% death within 5 years after surgery at stage I. Adjuvant chemotherapy is presently considered as a standard of care since beneficial effects have been demonstrated in stages IIA to IIIA (23). However, some controversies still exist over the impact of adjuvant

chemotherapy in stage IB (24, 25). Based on a gene expression profile called the lung metagene model, Potti et al has identified a subgroup of patients with stage IA disease who were at high risk for recurrence (26), thereby indicating that stage I NSCLC might represent heterogeneous prognostic subgroups. Recently, acetylation of H3K9 was reported to predict outcome of patients with stage I adenocarcinoma (27). In this study we demonstrate that loss of histone H4K20 trimethylation correlates with a poor survival for stage I adenocarcinoma patients. Altogether these data indicate that histone modifications might represent useful genomic tools to identify prognostic subgroups of patients that could justify the use of adjuvant chemotherapy, and suggest that analysis of combined histone modifications may help to better define prognostic subgroups. Further prospective studies are now required to evaluate their predictive power to chemosensitivity.

References

1. Pogribny IP, Ross SA, Tryndyak VP, Pogribna M, Poirier LA, Karpinets TV. Histone H3 lysine 9 and H4 lysine 20 trimethylation and the expression of Suv4-20h2 and Suv-39h1 histone methyltransferases in hepatocarcinogenesis induced by methyl deficiency in rats. Carcinogenesis 2006;27: 1180-6.

2. Hoffman PC, Mauer AM, Vokes EE. Lung cancer. Lancet 2000;355: 479-85.

3. Spira A, Ettinger DS. Multidisciplinary management of lung cancer. N Engl J Med 2004;350: 379-92.

4. Mao L, Lee JS, Kurie JM*, et al.* Clonal genetic alterations in the lungs of current and former smokers. J Natl Cancer Inst 1997;89: 857-62.

5. Osada H, Takahashi T. Genetic alterations of multiple tumor suppressors and oncogenes in the carcinogenesis and progression of lung cancer. Oncogene 2002;21: 7421-34.

6. Shames DS, Girard L, Gao B*, et al.* A genome-wide screen for promoter methylation in lung cancer identifies novel methylation markers for multiple malignancies. PLoS Med 2006;3: e486.

7. Bowman RV, Yang IA, Semmler AB, Fong KM. Epigenetics of lung cancer. Respirology 2006;11: 355-65.

8. Kerr KM, Galler JS, Hagen JA, Laird PW, Laird-Offringa IA. The role of DNA methylation in the development and progression of lung adenocarcinoma. Dis Markers 2007;23: 5-30.

9. Jenuwein T, Allis CD. Translating the histone code. Science 2001;293: 1074-80.

10. Groth A, Rocha W, Verreault A, Almouzni G. Chromatin challenges during DNA replication and repair. Cell 2007;128: 721-33.

11. Li B, Carey M, Workman JL. The role of chromatin during transcription. Cell 2007;128: 707-19.
12. Kouzarides T. Chromatin modifications and their function. Cell 2007;128: 693-705.
13. Seligson DB, Horvath S, Shi T*, et al.* Global histone modification patterns predict risk of prostate cancer recurrence. Nature 2005;435: 1262-6.
14. Fraga MF, Ballestar E, Villar-Garea A*, et al.* Loss of acetylation at Lys16 and trimethylation at Lys20 of histone H4 is a common hallmark of human cancer. Nat Genet 2005;37: 391-400.
15. Tryndyak VP, Kovalchuk O, Pogribny IP. Loss of DNA methylation and histone H4 lysine 20 trimethylation in human breast cancer cells is associated with aberrant expression of DNA methyltransferase 1, Suv4-20h2 histone methyltransferase and methyl-binding proteins. Cancer Biol Ther 2006;5: 65-70.
16. Beasley MB, Brambilla E, Travis WD. The 2004 World Health Organization classification of lung tumors. Semin Roentgenol 2005;40: 90-7.
17. Schemper M, Smith TL. A note on quantifying follow-up in studies of failure time. Control Clin Trials 1996;17: 343-6.
18. Eymin B, Gazzeri S, Brambilla C, Brambilla E. Mdm2 overexpression and p14(ARF) inactivation are two mutually exclusive events in primary human lung tumors. Oncogene 2002;21: 2750-61.
19. Guccione E, Bassi C, Casadio F*, et al.* Methylation of histone H3R2 by PRMT6 and H3K4 by an MLL complex are mutually exclusive. Nature 2007;449: 933-7.
20. Kirmizis A, Santos-Rosa H, Penkett CJ*, et al.* Arginine methylation at histone H3R2 controls deposition of H3K4 trimethylation. Nature 2007;449: 928-32.
21. Auerbach O, Hammond EC, Garfinkel L. Changes in bronchial epithelium in relation to cigarette smoking, 1955-1960 vs. 1970-1977. N Engl J Med 1979;300: 381-5.
22. Schotta G, Lachner M, Sarma K*, et al.* A silencing pathway to induce H3-K9 and H4-K20 trimethylation at constitutive heterochromatin. Genes Dev 2004;18: 1251-62.
23. Arriagada R, Bergman B, Dunant A, Le Chevalier T, Pignon JP, Vansteenkiste J. Cisplatin-based adjuvant chemotherapy in patients with completely resected non-small-cell lung cancer. N Engl J Med 2004;350: 351-60.
24. Winton T, Livingston R, Johnson D*, et al.* Vinorelbine plus cisplatin vs. observation in resected non-small-cell lung cancer. N Engl J Med 2005;352: 2589-97.
25. rosell R dlm, carpagnano f, ramlau r, gonzalez-larriba j, grodzki t, le groumellec a, aubet d, gasmi j, douillard j. ANITA: phase III adjuvant vinorelbine (N) and cisplatin (P) versus observation in completely resected (stageI-III) non small cell lung cancer (NSCLC) patients (pts). Lung Cancer 2005;49.
26. Potti A, Mukherjee S, Petersen R*, et al.* A genomic strategy to refine prognosis in early-stage non-small-cell lung cancer. N Engl J Med 2006;355: 570-80.
27. Barlesi F, Giaccone G, Gallegos-Ruiz MI*, et al.* Global histone modifications predict prognosis of resected non small-cell lung cancer. J Clin Oncol 2007;25: 4358-64.

Acknowledgments

We thank Pascal Perron, Céline Lampréia, Laurence David-Boudet and Sylvie Veyrenc for technical assistance.

Figure legends

Figure 1 Global modification of histone H4 acetylation in lung tumors

Left panel: immunostaining of lung cancer tissue on frozen sections using anti-acetylated H4K5, H4K8, H4K12 and H4K16 antibodies (immunoperoxidase, X200). Strong nuclear staining of acetylated H4K5 (a) and H4K8 (b) in squamous cell carcinoma. Low nuclear staining of acetylated H4K12 (c) and H4K16 (d) in squamous cell carcinoma and adenocarcinoma respectively. Middle panel: representative western blots showing high level of acetylated H4K5/K8 and low level of acetylated H4K12/K16 in lung tumors as compared to their matched normal lung tissues. Hybridization with actin antibody was used as a loading control. Right panel: distribution of staining for the four antibodies across all the 100 tumor samples. The y-axis is the fraction of samples showing the indicated score of staining (x axis).

Figure 2 Distribution of H4K5Ac, H4K8Ac, H4K12Ac and H4K16Ac staining scores according to histological type of lung tumors. Statistical analyses were performed using a Mann-Whitney test.

Figure 3 Global modification of H4K20 trimethylation in lung tumors.

A, Immunostaining of norma1 lung parenchyma and lung cancer tissue on frozen sections using anti-trimethylated H4K20 antibody. (immunoperoxidase, X200) (a). Strong nuclear staining of trimethylated H4K20 is observed in normal lung parenchyma, (b). Loss of H4K20me3 staining in an adenocarcinoma B, Representative western blot showing decreased expression of trimethylated H4K20 in lung tumors as compared to their matched normal lung

tissues. Hybridization with actin antibody was used as a loading control. C, Distribution of H4K20me3 staining across all the 100 tumor samples. The y-axis is the fraction of samples showing the indicated score of staining (x axis). D, Distribution of H4K20me3 scores according to histological type of lung tumors. Statistical analysis was performed using a Mann-Whitney test.

Figure 4 Modification of H4K20 trimethylation in squamous preinvasive lesions

A, Distribution of H4K20me3 staining across squamous cell carcinoma. The y-axis is the fraction of samples showing the indicated score of staining (x axis). B, Distribution of H4K20me3 staining across squamous preinvasive lesions. The y-axis is the score of H4K20me3 staining for the indicated preinvasive lesions (x axis). N, normal lung; H, hyperplasia; M, metaplasia; miD, mild dysplasia; moD, moderate dysplasia; sD, severe dysplasia; CIS, carcinoma in situ. C, Immunostaining on frozen sections of squamous preneoplasia from patient 7 using anti trimethylated H4K20 antibody. (a), strong nuclear immunostaining in normal bronchial epithelium. (b), immunostaining in hyperplastic bronchial epithelium. Note the absence of staining in some suprabasal cells. (c), immunostaining in a moderate dysplasia surrounded by severe dysplasia. Note the strong positive staining of epithelial cells above dysplastic cell. (d), immunostaining in a severe dysplasia. (e), immunostaining in CIS. (f), immunostaining in invasive carcinoma. (a,f), immunoperoxidase staining, X200.

Figure 5 H4K20me3 influences survival of patients with stage I adenocarcinoma

A, tested series of 23 stage I ADC patients, B, validation series of 57 independent stage I ADC patients, C, global population of stage I ADC patients combining test series and validation cases (80 cases). A,B,C left panel, distribution of H4K20me3 staining identifies

two groups of tumors with low (≤100) or high (>100) H4K20me3 score. The y-axis is the fraction of samples showing the indicated score of staining (x axis). Right panel, Kaplan-Meier analysis recording cancer related death of the two groups of patients according to high (>100) or low (≤100) H4K20me3 score.

Table1. Correlation between H4K20me3 and Suv4-20h1/2 status in lung tumors

		Suv4-20h1**			Suv4-20h2**		
		Nl	low		Nl	low	
H4K20me3*	high	6	9	p = 0.37	10	5	p = 0.019
	low	4	12		4	12	

*Immunohistochemical score, high ≥210, low ≤60, ** expression level according RT-QPCR; NL, Normal, low ≤50, Chi

Figure 1

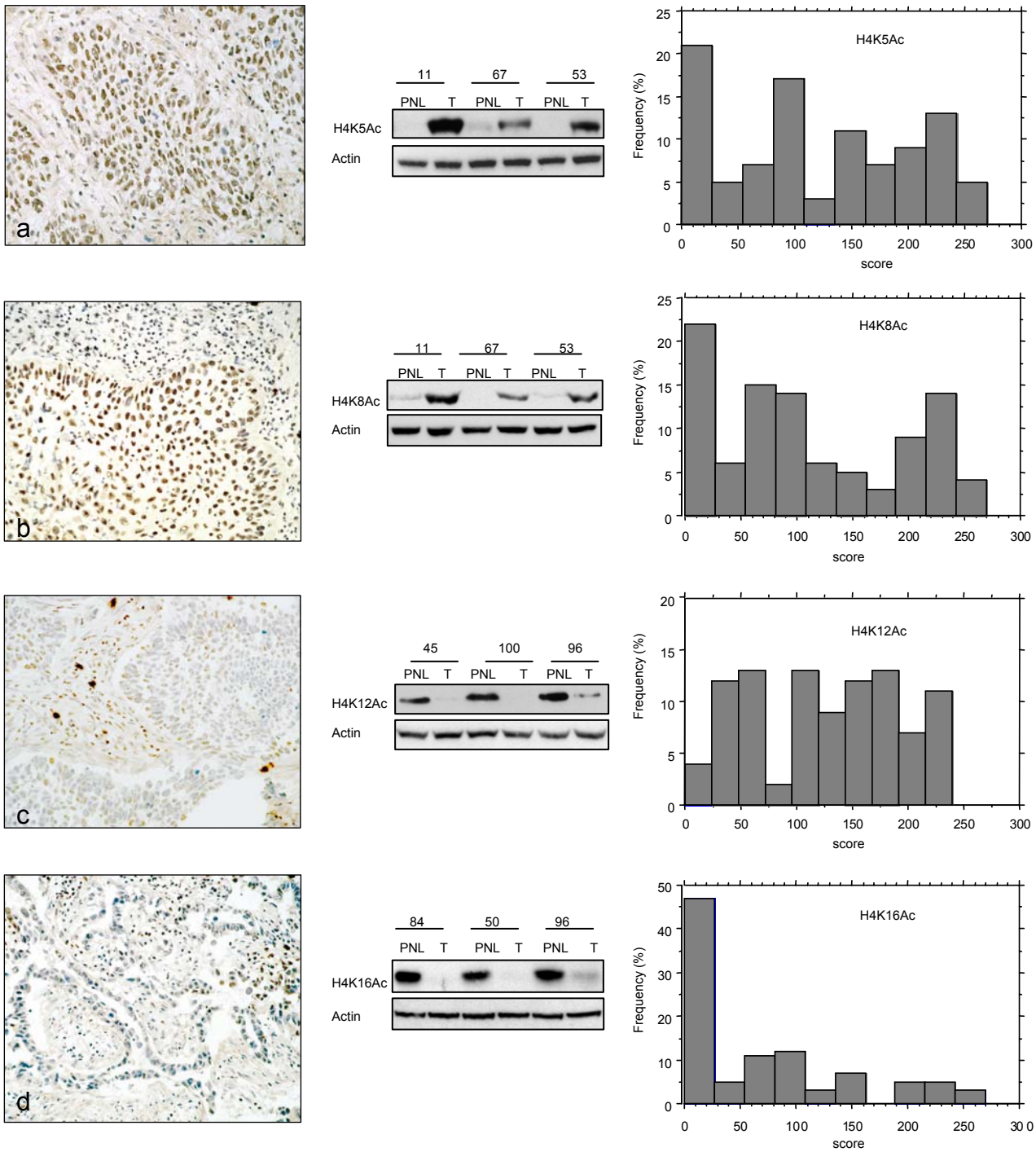
a
11
67
53
PNL T PNL T PNL T
H4K5Ac
Actin
H4K5Ac
Frequency (%)
score
b
H4K8Ac
Actin
H4K8Ac
c
45
100
96
H4K12Ac
Actin
H4K12Ac
d
84
50
96
H4K16Ac
Actin
H4K16Ac

Figure 2

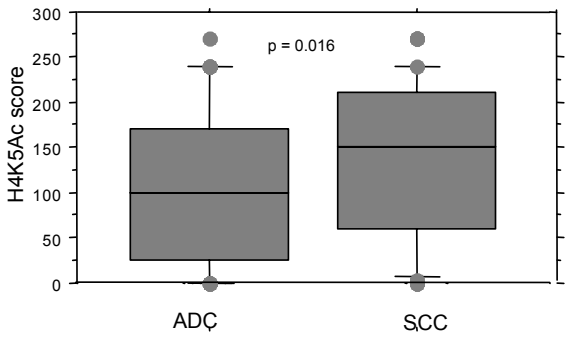
H4K5Ac score
300
250
200
150
100
50
0
p = 0.016
ADÇ
SCC

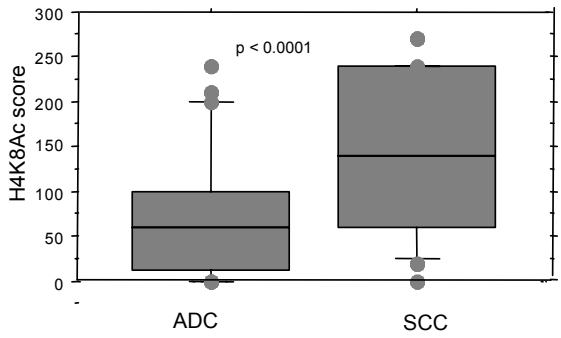
H4K8Ac score
300
250
200
150
100
50
0
p < 0.0001
ADC
SCC

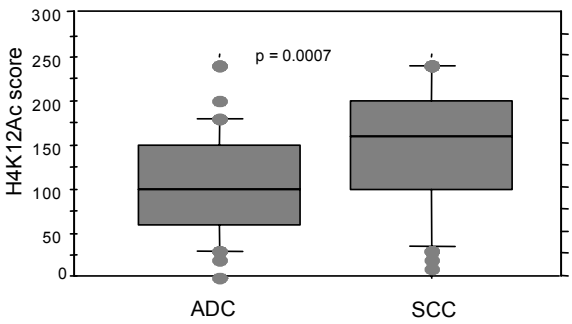
H4K12Ac score
300
250
200
150
100
50
0
p = 0.0007
ADC
SCC

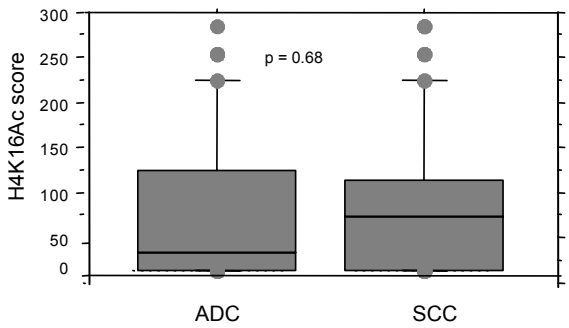
H4K16Ac score
300
250
200
150
100
50
0
p = 0.68
ADC
SCC

Figure 3

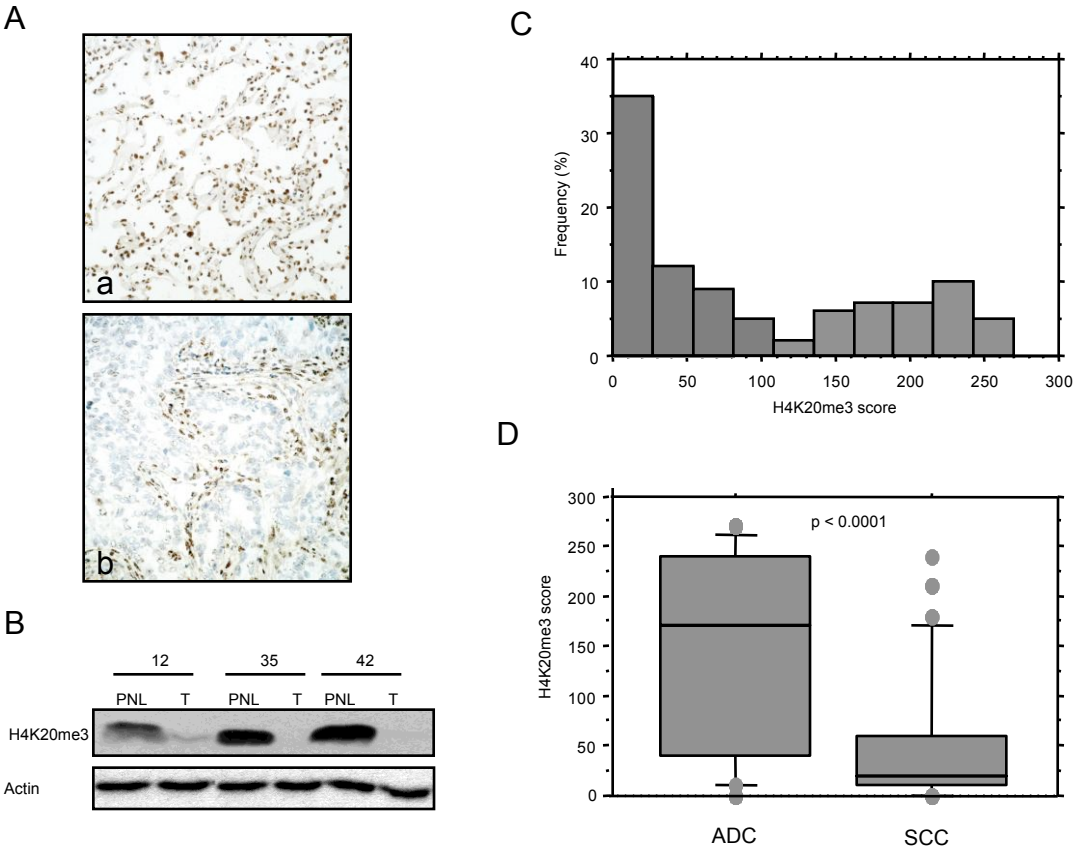
A
a
b
B
12
35
42
PNL
T
PNL
T
PNL
T
H4K20me3
Actin
C
Frequency (%)
H4K20me3 score
D
H4K20me3 score
p < 0.0001
ADC
SCC

Figure 4

A

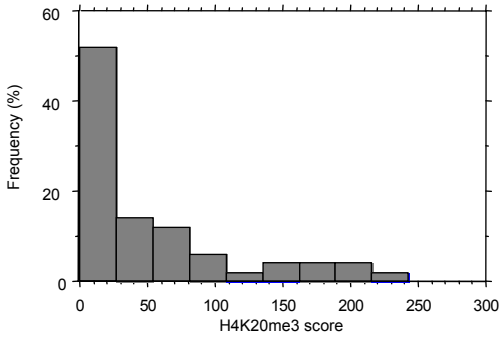
Frequency (%)
60
40
20
0
0
50
100
150
200
250
300
H4K20me3 score

B

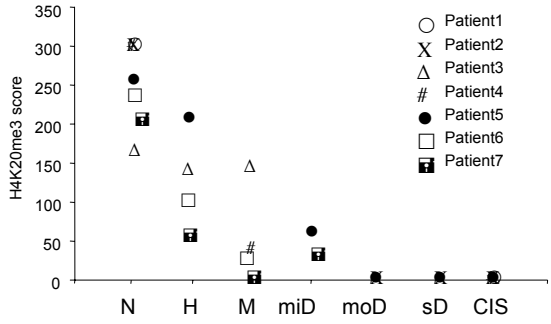
H4K20me3 score
350
300
250
200
150
100
50
0
N
H
M
miD
moD
sD
CIS
Patient1
Patient2
Patient3
Patient4
Patient5
Patient6
Patient7

C

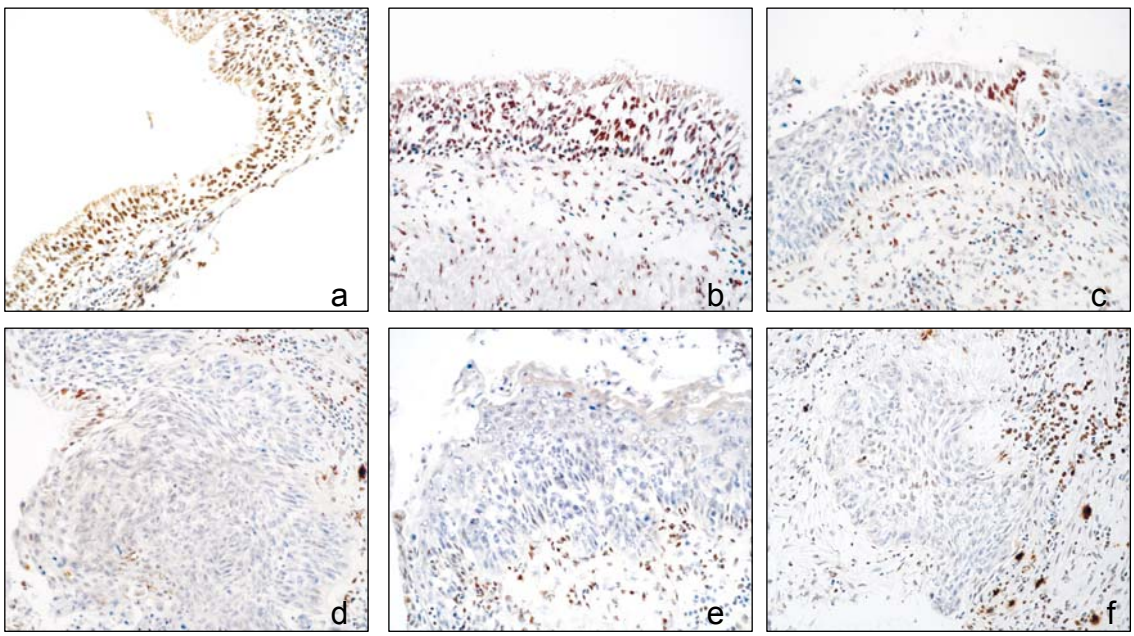
a
b
c
d
e
f

Figure 5

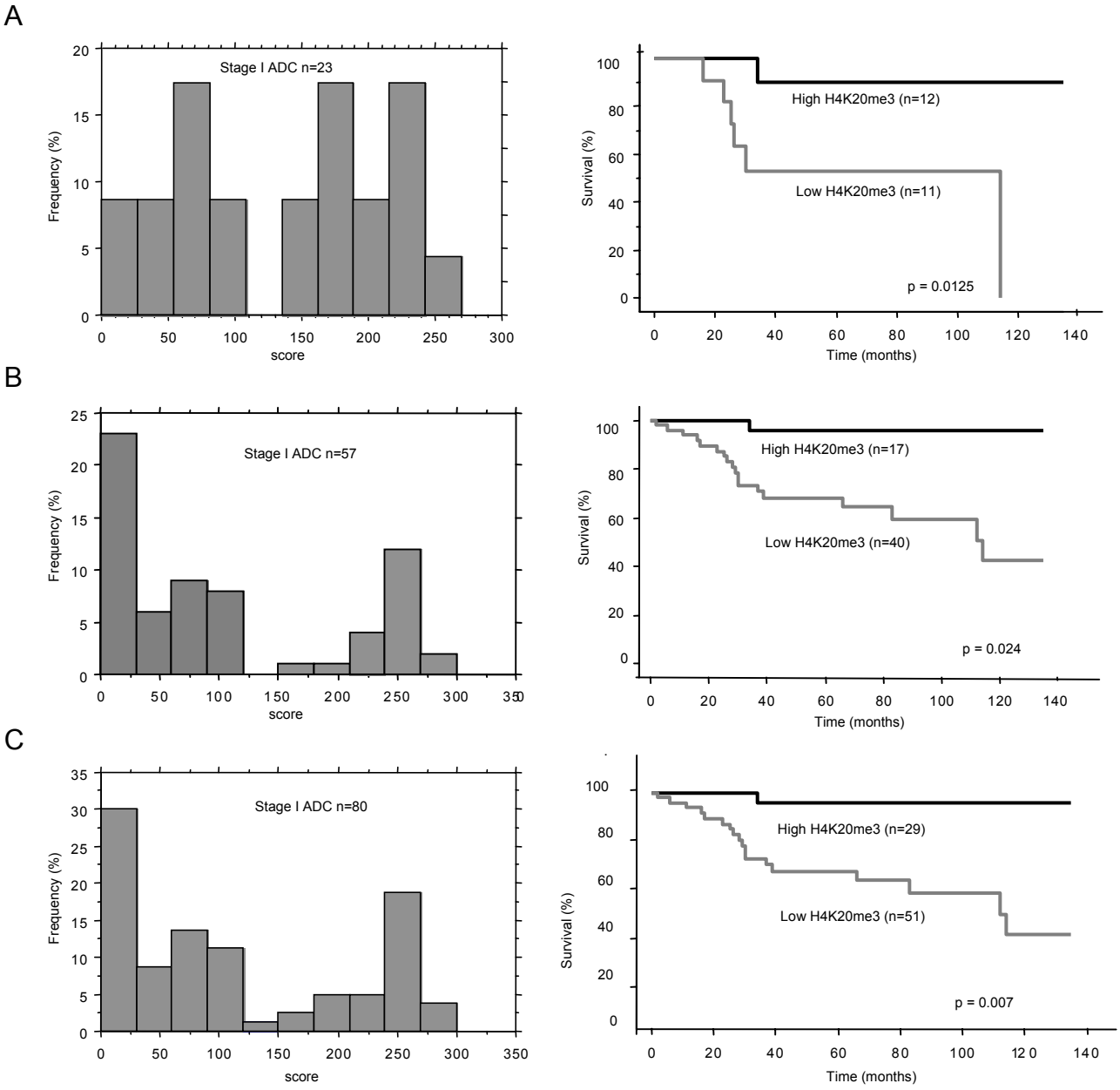
A
Stage I ADC n=23
Frequency (%)
score
High H4K20me3 (n=12)
Low H4K20me3 (n=11)
p = 0.0125
Survival (%)
Time (months)
B
Stage I ADC n=57
Frequency (%)
score
High H4K20me3 (n=17)
Low H4K20me3 (n=40)
p = 0.024
Survival (%)
Time (months)
C
Stage I ADC n=80
Frequency (%)
score
High H4K20me3 (n=29)
Low H4K20me3 (n=51)
p = 0.007
Survival (%)
Time (months)